

# Using $^{210}\text{Pb}$ Simulations for model Comparison and analysing

Marco A Aquino-López<sup>\*†</sup>

Nicole K. Sanderson<sup>‡</sup>

Maarten Blaauw<sup>§</sup>

J Andrés Christen<sup>¶</sup>

## Abstract

To understand changes in peat accumulation in response to recent and rapid climate or anthropogenic change, accurate ages for the last 100-200 years are essential. Dating this period is often complicated by poor resolution and large errors associated with calibrating radiocarbon ( $^{14}\text{C}$ ) ages. The use of lead-210 ( $^{210}\text{Pb}$ ) is a popular method as it allows for the measurement of absolute and continuous dates for the last 150 years of peat accumulation. In ombrotrophic peatlands, the lead-210 dating method has traditionally relied on the Constant Rate of Supply (CRS) model which uses the radioactive decay equation to provide a logarithmic model to approximate dates, resulting in a restrictive model. Key limitations of the CRS model are: (1) the accurate assessment of the supported lead which varies between sites and can be problematic if sampling of the total inventory is not continuous (e.g. interval measurements, lack of sample); (2) the inconsistent estimation of uncertainties. The Plum model was developed in a statistical framework with a Bayesian approach, notably resulting in longer chronologies, more realistic uncertainty estimations, and has the advantage of not double-modelling dates for final age-depth models, primarily radiocarbon and  $^{210}\text{Pb}$  chronologies. Here, we present two thorough tests of Plum. First, we created scenarios using simulated datasets with known age-depth functions in a range of shapes and with varying sampling resolution. These simulations are created using the physical behavior that most  $^{210}\text{Pb}$  dating models are based on. Plum and CRS model outputs are compared under each scenario. We also take this opportunity to demonstrate the new Plum's R package, for use by non-statisticians in palaeoecological studies. We also compare the lead-210 dates derived from CRS models and from Plum using real peat cores with additional independent dating controls from Eastern Canada. These cores represent a thorough test for Plum, as permafrost thaw drastically changes stratigraphy and peat type (e.g. shift from ligneous peat to Sphagnum moss) which affects  $^{210}\text{Pb}$  retention within the peat. Recent decadal-scale changes are still poorly represented so accurate dating is now essential to quantify changes in carbon accumulation rates and predict future trends.

**Keywords:** Chronology, Constant Rate of Supply, Plum, Simulations.

---

<sup>\*</sup>Centro de Investigación en Matemáticas (CIMAT), Jalisco s/n, Valenciana, 36023 Guanajuato, GT, Mexico.  
email: [aquino@cimat.mx](mailto:aquino@cimat.mx)

<sup>†</sup>Corresponding author.

<sup>‡</sup>College of Life and Environmental Sciences, University of Exeter, Exeter, EX4-4QJ. email: [N.K.Sanderson@exeter.ac.uk](mailto:N.K.Sanderson@exeter.ac.uk)

<sup>§</sup>School of Natural and Built Environment, Queen's University Belfast, Belfast, BT7-1NN.  
email: [maarten.blaauw@qub.ac.uk](mailto:maarten.blaauw@qub.ac.uk)

<sup>¶</sup>Centro de Investigación en Matemáticas (CIMAT), Jalisco s/n, Valenciana, 36023 Guanajuato, GT, Mexico.  
email: [jac@cimat.mx](mailto:jac@cimat.mx)

# 1 Introduction

## 2 Simulations

In order to observe the accuracy and precision of any model we need data to which we know the true age-depth function. Blaauw et al. (2018) presented a methodology for simulating radiocarbon dates and as their uncertainty, on the other hand Aquino-López et al. (2018) presented an approach for simulating  $^{210}\text{Pb}$  data given a age-depth function  $f(t)$ , it is important to note that this simulations follow the equations presented by Appleby and Oldfield (1978); Robbins (1978). By using the approach presented by Aquino-López et al. (2018) for obtaining  $^{210}\text{Pb}$  simulated data from and the uncertainty estimations presented by Blaauw et al. (2018), we can obtained resalable  $^{210}\text{Pb}$  simulated data.

For our simulations we constructed three different scenarios (see table 2), each with their own age-depth functions.

Label	Age-depth function	$\Phi$ ( $\frac{\text{Bq}}{\text{m}^2\text{yr}}$ )	Supported $^{210}\text{Pb}$ ( $\frac{\text{Bq}}{\text{kg}}$ )
Simulation 1	$\frac{x^2}{4} + \frac{x}{2}$	100	10
Simulation 2	$12x - .2x^2$	50	25
Simulation 3	$8x + 25 \sin(\frac{x}{\pi})$	500	15

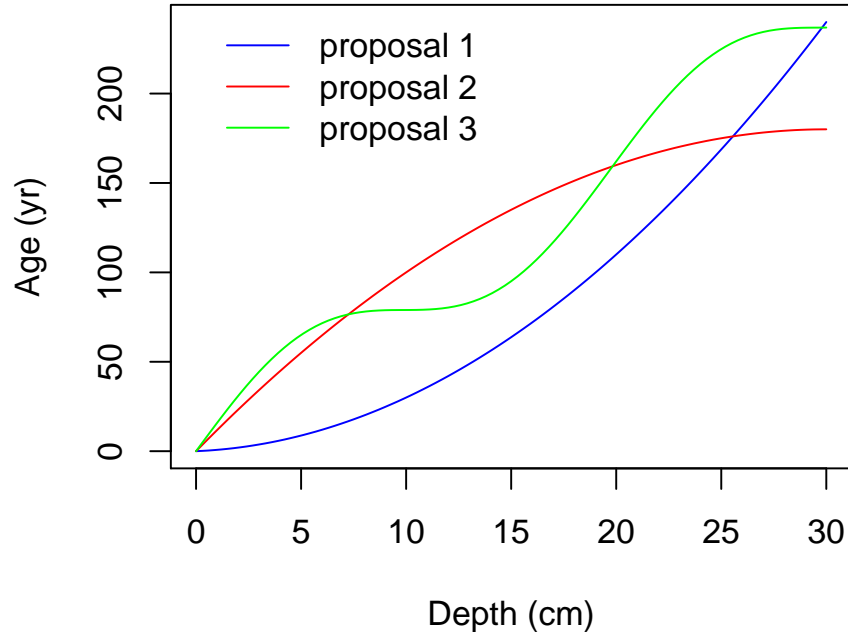
Table 1: Simulated age-depth function and parameters used in each simulation

Using the age-depth functions, defined in table 2, we can obtained simulate the activity at any depth or interval (by integrating the curve in such interval).

These concentrations can be interpreted as error-free measurements. Because every equipment is subject to error, we need to replicate this measurement errors. (Blaauw et al., 2018) presents error structure for radiocarbon dates. We can use this structure to our  $^{210}\text{Pb}$  measurements as both measurements are subject to similar measurement problems.

Let  $C_{\hat{x}}$  be the true  $^{210}\text{Pb}$  concentration in the interval  $\hat{x} = [a, b)$ , given the age-depth function  $t(x)$ . To simulate disturbances in the material, we can introduce scatter centred around the true value,  $C \sim \mathcal{N}(C_{\hat{x}}, x_{scat}^2)$ , where  $x_{scat}^2$  is the amount of scatter for this variable (in this case  $x_{scat}^2 = 10$ ). Now, to replicate outliers, we define a shift from the true value ( $x_{shift}$ ), which occurs with a

## Postulated age–depth models



## Resulting $^{210}\text{Pb}$ profiles

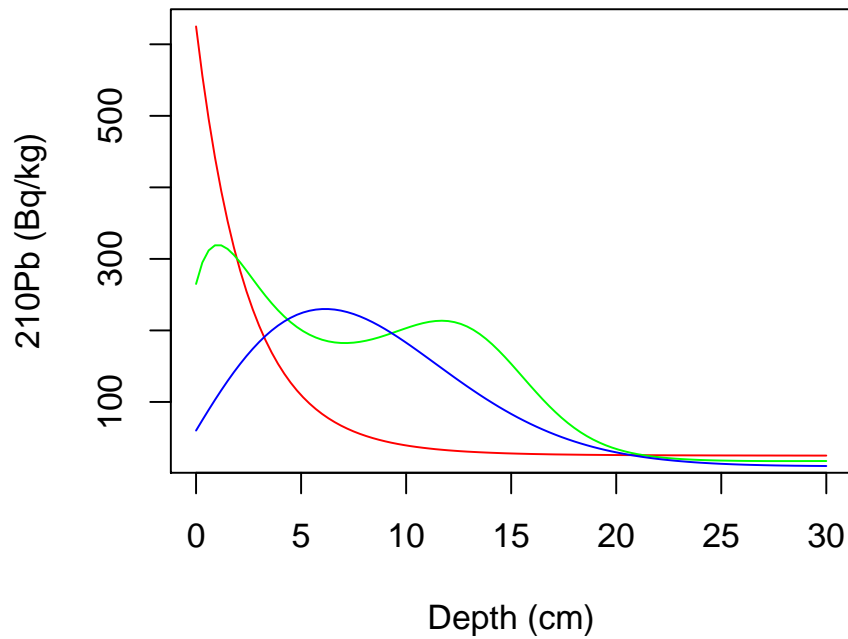


Figure 1: Proposed age–depth functions with their corresponding  $^{210}\text{Pb}$  profiles. Upper panel: Age–depth function for the three different proposals. Lower panel: Corresponding  $^{210}\text{Pb}$  profiles in relation to depth.

probability  $p_{out}$ . This results in a new variable  $\theta'$  which is defined as

$$\theta' = \begin{cases} \mathcal{U}(\hat{x} - x_{shift}\theta + x_{shift}), & p_{out} \\ \theta, & 1 - p_{out} \end{cases}. \quad (1)$$

To simulate the uncertainty provided by the laboratory, we can define the simulated measurements as  $y(\theta') \sim \mathcal{N}(\mu(\theta'), \sigma^2)$ , where  $\sigma_R$  is the standard deviation reported by the laboratory. To simulate  $\sigma_R$  we use  $\sigma_R = \max(\sigma_{min}, \mu(\theta') \varepsilon y_{scat})$ , where  $\sigma_{min}$  is the minimum standard deviation assigned to a measurement. This variable differs between laboratories (we will be using a default value of 1 Bq/kg). Finally,  $\varepsilon$  is the analytical uncertainty (default .01) and  $y_{scat}$  an error multiplier (default 1.5).

For this study we created a data set for each simulation by integrating in intervals of 1 cm from depth 0 to 30 (where equilibrium was guaranteed). The complete data sets can be found in the Supplementary Material 5 and Figure 1  $^{210}\text{Pb}$  concentrations curves.

With these base data sets, we then define a new variable call percentage of information. This variable relates to how many much of the available information was measured. For this we assumed that background was reached at depth  $m$ , information percentage is define as how much area of the core was measured, e.g. if background was reached at depth 100 cm and the core was sampled every 1 cm if 20 samples are measured, the percentage of information would be 20 %. This variable will help us to have a measuring tool for how many samples are needed for a good chronology without depending on the size of the samples.

### 3 Model Comparison

In order to compare both the CRS and Plum under similar circumstances the previously described data sets will be randomly selected for samples given a information percentage, e.g. for a percentage information of 50% given our 30 sample data set, 14 samples will randomly selected from the samples at depths 1 to 29, and the samples at depth 30 will be always included. This was done to guaranty that background is reached, which is required for the CRS model. In the case of cores which have not reach background, *Plum* (Aquino-López et al., 2018) has shown to provide accurate results without the need of user interference, the CRS can provide a chronology if inventory is completed, which means user innervation. To avoid this problem and to provide a more objective comparison every sampling set will have reach background.

### 3.1 Sampling Techniques

In order to observe how sampling affects the accuracy and precision of  $^{210}\text{Pb}$  models, we used the three simulated data sets created for the previous section. This simulated cores were randomly selected given a percentage of information (e.g. for a 20% information sample, in the 30 cm cores, 6 random samples were selected). Because the CRS model assumes that background has been reached, we decided to fix the last sample (30 cm depth) for every case, this will facilitate the CRS to provide more accurate results and also gives the model a single last depth to be removed as it is common practice when using this model. 100 individual samples were selected for information percentage from 10% to 90% in 5% intervals (e.i 10%, 15%, 20%,...,85% and 90%). After a random sample was selected both the CRS model and Plum were performed and compared to the true age value to calculate its accuracy.

In order to observe the precision and accuracy we decided to calculate the mean of length of the 95% intervals (in yr), the offset (in yr) as well as the normalized accuracy (this variable will show us how far the model is from the true value given its uncertainty).

From Figure 2, we can observe similar results those presented by Blaauw et al. (2018). The classical model (CRS) at first appears to provide a similar result (similar offset) to the Bayesian alternative (*Plum*) with a more precise result (if we only look at the length of the 95% interval). These results can be misleading if we don't analyse the effects of these two parameters in conjunction (offset and length of interval). In order to observe how well the model captures the true ages calculated the normal offset (see Figure 2). These figures show how on average the models contain the true within their uncertainty intervals (normalized to one standard deviation). Any value which is over the second standard deviations represents that the model is incapable of capturing the true ages within their uncertainty intervals. This means that the CRS provides small uncertainties at the cost of its accuracy. It also appears that the length of the 95% interval and offset is not affected by how much information is provided to the model. This is a result of the use of interpolation used by the method.

On the other hand, *Plum*, which is a Bayesian method, shows more accurate results as more information is given to the model, this is similar to the ones found by Blaauw et al. (2018). When we observe the regular offset (not normalized), we observed that Plum provides a much smaller offset in comparison to the CRS model, this in combination with slightly bigger uncertainties results in a consistently accurate model which is capable of capturing the true values within its uncertainty

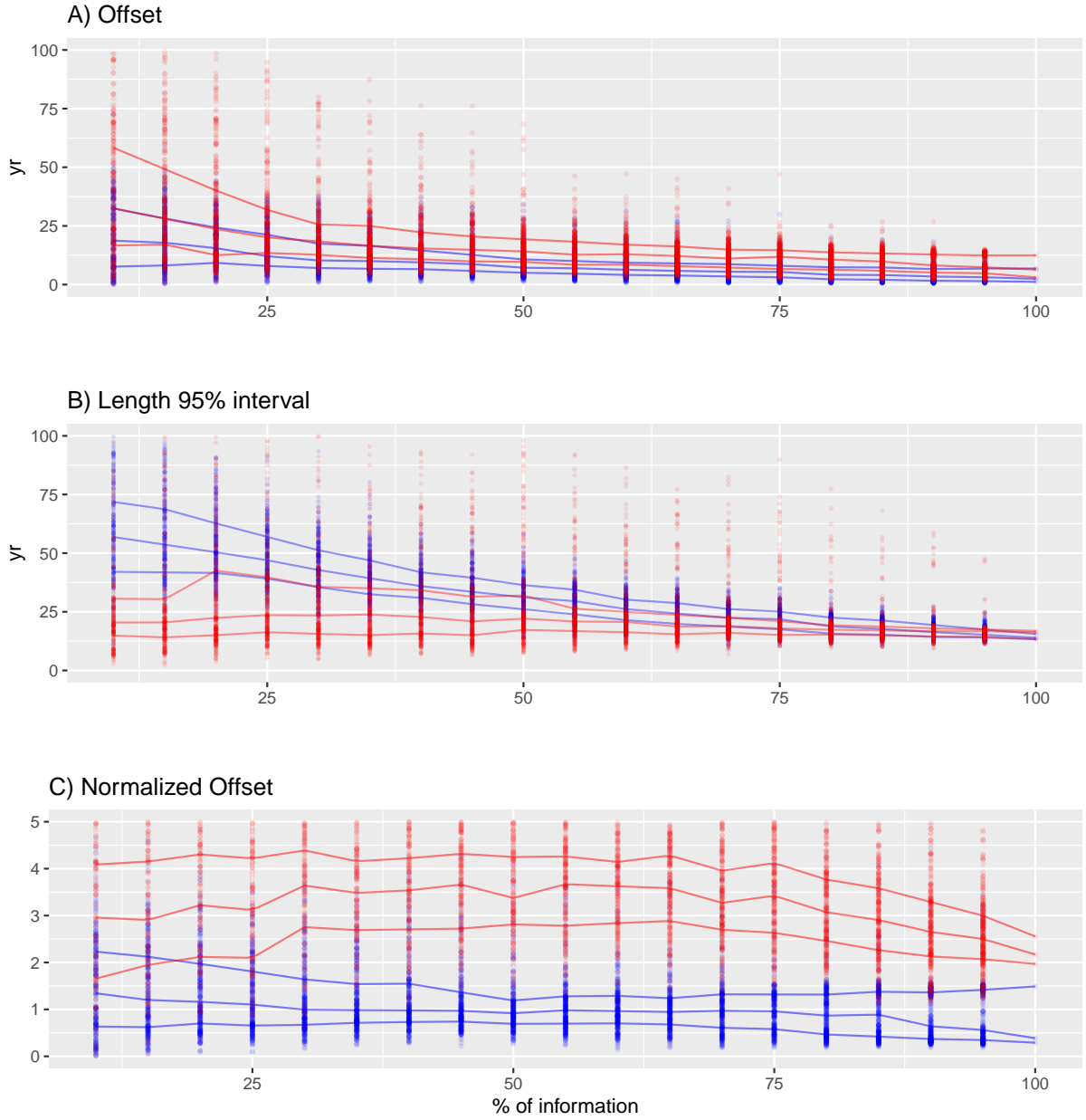


Figure 2: Comparison of the offset (distance between the true age and model), the length of the 95% confidence interval (classical) and credible interval (Bayesian) and the Normalized offset between the classical CRS model vs the Bayesian approach *Plum*. Top panel A) shows the offset between the true age and modelled age of the CRS (red) and *Plum* (blue). Middle panel B) length of the 95% confidence interval for the CRS model (in red) and the 95% credible interval of *Plum* (in blue). Bottom panel C) Normalized offset presenting the distance between the modelled age and the true age normalized divided by the standard deviation (in the case of *Plum*, the length of the interval divided by 4), CRS in red and *Plum* in blue.

intervals. This result supports the claim that *Plum* provides more realistic uncertainties when compared to the CRS.

Plum has 87.86% (4686/5333) of its runs under the 2 standard deviations, on the other hand the CRS model only has 7.48% (399/5333). We can also observe a clear structure on the way Plum increases its accuracy and precision to obtain a better chronology, on the side the CRS model appears to not have this structure.

## 4 Conclusions and Discussion

### References

- Appleby, P. and Oldfield, F. (1978). The calculation of lead-210 dates assuming a constant rate of supply of unsupported 210pb to the sediment. *Catena*, 5(1):1–8.
- Aquino-López, M. A., Blaauw, M., Christen, J. A., and Sanderson, N. K. (2018). Bayesian analysis of 210pb dating. *Journal of Agricultural, Biological and Environmental Statistics*, 23(3):317–333.
- Blaauw, M., Christen, J. A., Bennett, K., and Reimer, P. J. (2018). Double the dates and go for Bayes — impacts of model choice, dating density and quality on chronologies. *Quaternary Science Reviews*, 188:58–66.
- Robbins, J. (1978). Geochemical and geophysical applications of radioactive lead. *The biogeochemistry of lead in the environment*, pages 285–393.

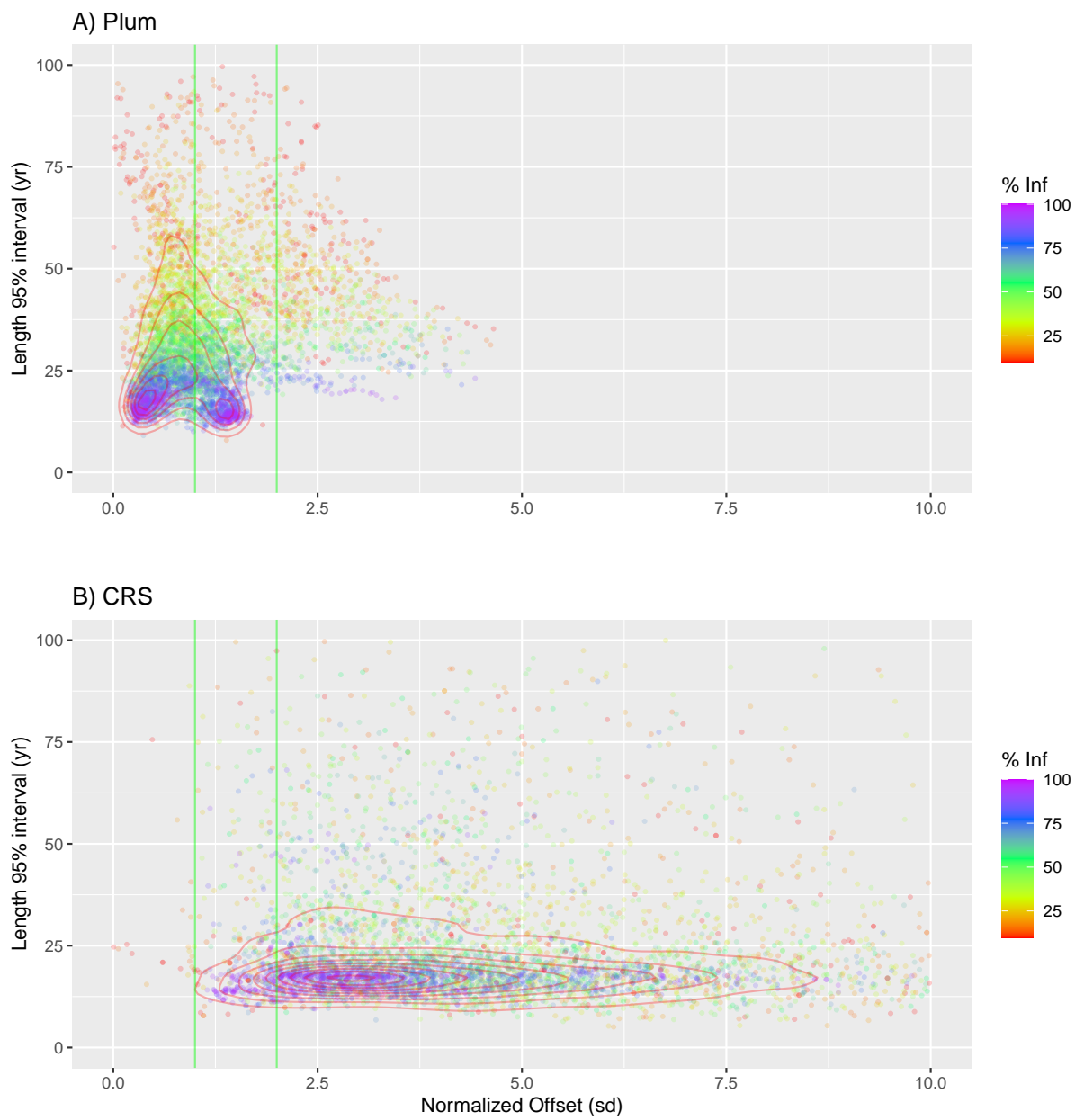


Figure 3:



## 5 Supplementary Material

Label	Depth (cm)	Density ( $g/cm^3$ )	210Pb (Bq/kg)	sd(210Pb)	Thickness (cm)	226Ra (Bq/kg)	sd(226Ra)
Sim01-01	1	0.10009	63.50103	2.85755	1	23.8045	1.125
Sim01-02	2	0.10064	80.08738	3.60393	1	23.2924	1.125
Sim01-03	3	0.10173	98.32806	4.42476	1	23.434	1.125
Sim01-04	4	0.10334	125.45705	5.64557	1	26.0873	1.125
Sim01-05	5	0.10547	141.27971	6.35759	1	22.8041	1.125
Sim01-06	6	0.10809	130.27571	5.86241	1	23.4333	1.125
Sim01-07	7	0.11116	134.04051	6.03182	1	25.6156	1.125
Sim01-08	8	0.11466	129.69245	5.83616	1	26.1371	1.125
Sim01-09	9	0.11855	134.93655	6.07214	1	25.4813	1.125
Sim01-10	10	0.12278	109.39886	4.92295	1	25.8877	1.125
Sim01-11	11	0.12731	110.68133	4.98066	1	24.4414	1.125
Sim01-12	12	0.13209	102.38094	4.60714	1	24.9053	1.125
Sim01-13	13	0.13706	75.80895	3.4114	1	22.9151	1.125
Sim01-14	14	0.14218	77.60406	3.49218	1	24.4808	1.125
Sim01-15	15	0.14738	68.4401	3.0798	1	24.9343	1.125
Sim01-16	16	0.15262	60.72037	2.73242	1	25.2659	1.125
Sim01-17	17	0.15782	50.28147	2.26267	1	22.961	1.125
Sim01-18	18	0.16294	44.24641	1.99109	1	22.9139	1.125
Sim01-19	19	0.16791	39.85997	1.7937	1	28.3774	1.125
Sim01-20	20	0.17269	38.40823	1.72837	1	23.5379	1.125
Sim01-21	21	0.17722	32.75922	1.47416	1	25.4363	1.125
Sim01-22	22	0.18145	28.02545	1.26115	1	24.8995	1.125
Sim01-23	23	0.18534	27.8749	1.25437	1	22.6783	1.125
Sim01-24	24	0.18884	30.74797	1.38366	1	24.8575	1.125
Sim01-25	25	0.19191	28.36187	1.27628	1	24.8724	1.125
Sim01-26	26	0.19453	27.24535	1.22604	1	24.3778	1.125
Sim01-27	27	0.19666	23.59236	1.06166	1	24.7209	1.125
Sim01-28	28	0.19827	25.74855	1.15868	1	24.6615	1.125
Sim01-29	29	0.19936	25.05368	1.12742	1	24.7199	1.125
Sim01-30	30	0.19991	25.0065	1.12529	1	24.4937	1.125

Label	Depth (cm)	Density ( $g/cm^3$ )	210Pb (Bq/kg)	sd(210Pb)	Thickness (cm)	226Ra (Bq/kg)	sd(226Ra)
Sim02-01	1	0.1001	909.3928	40.9227	1	8.9761	0.45
Sim02-02	2	0.1006	683.9989	30.7799	1	10.0607	0.45
Sim02-03	3	0.1017	453.0503	20.3873	1	9.8701	0.45
Sim02-04	4	0.1033	310.7897	13.9855	1	10.37	0.45
Sim02-05	5	0.1055	218.0058	9.8103	1	10.0418	0.45
Sim02-06	6	0.1081	158.6974	7.1414	1	10.104	0.45
Sim02-07	7	0.1112	113.9062	5.1258	1	10.2049	0.45
Sim02-08	8	0.1147	75.5493	3.3997	1	9.334	0.45
Sim02-09	9	0.1185	56.6252	2.5481	1	10.5145	0.45
Sim02-10	10	0.1228	44.1595	1.9872	1	9.8677	0.45
Sim02-11	11	0.1273	34.7448	1.5635	1	9.7694	0.45
Sim02-12	12	0.1321	25.384	1.1423	1	10.5134	0.45
Sim02-13	13	0.1371	24.0007	1.08	1	10.4589	0.45
Sim02-14	14	0.1422	21.3643	1	1	9.9504	0.45
Sim02-15	15	0.1474	17.7932	1	1	10.5135	0.45
Sim02-16	16	0.1526	15.0416	1	1	10.3362	0.45
Sim02-17	17	0.1578	14.2937	1	1	10.5131	0.45
Sim02-18	18	0.1629	12.3844	1	1	10.368	0.45
Sim02-19	19	0.1679	12.6023	1	1	10.5297	0.45
Sim02-20	20	0.1727	11.9329	1	1	10.0924	0.45
Sim02-21	21	0.1772	9.301	1	1	10.118	0.45
Sim02-22	22	0.1815	10.7777	1	1	10.249	0.45
Sim02-23	23	0.1853	12.9491	1	1	10.134	0.45
Sim02-24	24	0.1888	10.6571	1	1	10.1151	0.45
Sim02-25	25	0.1919	9.6297	1	1	9.6608	0.45
Sim02-26	26	0.1945	8.4331	1	1	8.7821	0.45
Sim02-27	27	0.1967	10.4921	1	1	9.8995	0.45
Sim02-28	28	0.1983	11.135	1	1	9.2481	0.45
Sim02-29	29	0.1994	10.109	1	1	10.4398	0.45
Sim02-30	30	0.1999	9.5404	1	1	10.1114	0.45

Label	Depth (cm)	Density ( $g/cm^3$ )	210Pb (Bq/kg)	sd(210Pb)	Thickness (cm)	226Ra (Bq/kg)	sd(226Ra)
Sim03-01	1	0.1001	6384.1354	287.2861	1	15.8007	0.675
Sim03-02	2	0.1006	3550.0809	159.7536	1	14.5245	0.675
Sim03-03	3	0.1017	1954.5702	87.9557	1	15.6527	0.675
Sim03-04	4	0.1033	1183.8917	53.2751	1	14.5175	0.675
Sim03-05	5	0.1055	760.2132	34.2096	1	14.9242	0.675
Sim03-06	6	0.1081	360.2553	16.2115	1	14.801	0.675
Sim03-07	7	0.1112	212.9402	9.5823	1	14.8738	0.675
Sim03-08	8	0.1147	104.2684	4.6921	1	14.9028	0.675
Sim03-09	9	0.1185	44.3849	1.9973	1	15.0768	0.675
Sim03-10	10	0.1228	18.6447	1	1	15.3764	0.675
Sim03-11	11	0.1273	23.2778	1.0475	1	14.6231	0.675
Sim03-12	12	0.1321	53.1587	2.3921	1	15.1629	0.675
Sim03-13	13	0.1371	97.363	4.3813	1	14.3047	0.675
Sim03-14	14	0.1422	116.9788	5.264	1	14.0261	0.675
Sim03-15	15	0.1474	153.2901	6.8981	1	15.9723	0.675
Sim03-16	16	0.1526	151.8496	6.8332	1	14.7579	0.675
Sim03-17	17	0.1578	136.3609	6.1362	1	16.114	0.675
Sim03-18	18	0.1629	107.2736	4.8273	1	15.4595	0.675
Sim03-19	19	0.1679	76.8966	3.4603	1	15.9439	0.675
Sim03-20	20	0.1727	48.9213	2.2015	1	14.6235	0.675
Sim03-21	21	0.1772	40.4439	1.82	1	14.6716	0.675
Sim03-22	22	0.1815	26.5638	1.1954	1	16.2541	0.675
Sim03-23	23	0.1853	21.714	1	1	14.4826	0.675
Sim03-24	24	0.1888	17.6428	1	1	15.5109	0.675
Sim03-25	25	0.1919	17.3533	1	1	13.6898	0.675
Sim03-26	26	0.1945	17.4211	1	1	14.4684	0.675
Sim03-27	27	0.1967	16.4246	1	1	15.3889	0.675
Sim03-28	28	0.1983	12.4828	1	1	15.0698	0.675
Sim03-29	29	0.1994	13.5514	1	1	15.2346	0.675
Sim03-30	30	0.1999	14.3145	1	1	14.7846	0.675